Functional Composite Materials

RESEARCH

Open Access

Molecular sieving through 'layer-by-layer' self-assembly of polyelectrolytes and highly crosslinked graphene oxide

Subhasish Maiti and Suryasarathi Bose[*]

Abstract

Lack of access to potable water and abating levels of ground water level demands the reuse of unconventional water sources after remediating it in a sustainable way. In this context, purifying brackish, land and sea water seems a feasible solution to the ever-growing population.

In this work, a novel composite membrane was fabricated by 'layer-by-layer' self-assembly of poly-dopamine (PDA) and polystyrene sulfonate (PSS) supported on a highly crosslinked graphene oxide (GO) membrane to sieve ions to purify contaminated water as well as enhance the resistance towards chlorine. This GO membrane was sandwiched between layers of various nanoporous polyvinylidene difluoride (PVDF) membranes obtained by selectively etching out the PMMA component from the demixed blends. The blend membranes were designed following the melt-extrusion process and subsequent quenching to facilitate confined crystallization of PVDF and selective etching of PMMA. The membranes with different pore sizes were tuned on varying the composition in blends and a gradient in microstructure was achieved by stitching the membranes. Pure water flux, salt rejection, dye removal, and antibacterial activity were performed to study the membrane's efficiency. The GO membrane was chemically crosslinked with methylenediamine to impart dimensional stability and to enhance rejection efficiency through the nanoslits that GO offers. Besides effective rejection, the sandwiched membrane was modified with 'layer-by-layer' self-assembly of polyelectrolytes on the surface to improve the chlorine tolerance performance. This strategy resulted in an excellent salt (about 95% and 97% for monovalent and divalent ion, respectively) and dye rejection (100% for both cationic and anionic dye), besides facilitating excellent chlorine tolerance performance. Moreover, this modified membrane showed superior antifouling properties (flux recovery ratio is more than 90%) and excellent antibacterial performance (near about 3 log reduction).

Thus the concept of using layer-by-layer self-assembly of polycations (PDA) and polyanions (PSS) onto a hierarchical chemically modified GO sandwiched PVDF membrane proved to be a productive strategy to purify contaminated water. Thus the membrane can be a potential candidate for domestic as well as industrial application.

Keywords: PVDF membranes, Self-assembly, Polyelectrolytes, Chemically crosslinked GO, Selective rejection, Chlorine resistance, Antibacterial

Introduction

With the increasing population, there is an acute shortage of groundwater. This demands more efficient water purification technologies to purify land and seawater and make them fit for drinking [1, 2]. The membrane-based technology has received significant attention as it is economically viable and easy to deploy on industrial scale

*Correspondence: sbose@iisc.ac.in

Department of Materials Engineering, Indian Institute of Science, Bangalore, Karnataka 560012, India

[3–5]. Therefore, in this context, membrane technology, particularly the use of polymeric membranes, is highly desirable because of its cost-effectiveness and ease of upscaling. The overall cost can be minimized by utilizing less energy-intensive techniques like Forward Osmosis (FO) [6–10]. FO is essentially a process via which separation can be carried out, and it is driven by natural osmotic pressure, which further eliminates any additional pumping cost. In this context, less energy-intensive, minimal fouling tendency and easy recovery of fresh water from draw solutions are the main characteristics that make FO more attractive [11–14].

Polyamide (PA)-based both RO and FO membranes are well-known in the literature for their better sieving performance. A significant bottleneck towards the application of PA membranes' are their susceptibility to chlorine attack. The amide linkages usually disintegrate when exposed to chlorine atmosphere [15]. However, various carbon-based materials such as MXene [16, 17], graphene [18], carbon dots [19], GO [20], GQD [21], CNT [22] modified PA membrane are extensively used to improve the chlorine tolerance performance. Among these, GO embedded PA-based TFC membrane [23] showed some promise. However, incorporating a large quantity of GO into the PA layer is a limitation because it tends to block the pores that affect water flux. Therefore, challenges still exist to fabricate membranes with excellent rejection without suppressing other essential membrane parameters such as water flux, chlorine tolerance, antifouling, and antibacterial performance. Another disadvantage of pristine GO is it swells in an aqueous environment [24]. Some modifications on GO have been reported in the literature to stabilize it underwater; most of them are used for different application [25–28].

Layer-by-layer assembly is an excellent strategy, and it has been widely used to fabricate thin-film composite membranes by alternatively adsorbing polycations and polyanions [29]. Therefore better water flux is expected compared to the PA-TFC membrane. Moreover, the surface charge species can be easily tailored according to the various application by choosing the suitable layer. Another main advantage of this strategy is that it can provide more binding sites, an essential requirement to achieve molecular sieving [30].

In this work, a unique strategy was adopted to target two key attributes related to membrane performance; sieving ions and chlorine tolerance. To achieve this, layers of nanoporous membranes, derived by selectively etching the PMMA component from the demixed PVDF/PMMA blend, were stacked using an adhesive to design a gradient in pore morphology. Blends of PVDF and PMMA- a model UCST system, were chosen here. Allowing the blends to phase separate below the UCST temperature followed by selective etching of the PMMA phase, various nanoporous membranes were developed. The PMMA component, restricted in either the interspheruitic regions or interlamellar regions, was selectively etched out to yield nanochannels. Polyacrylic acid (PAA) was used to stitch different membranes and hence a hierarchical porous structure was designed. A highly crosslinked GO membrane was then sandwiched, followed by creating an active surface through the layer-by-layer assembly of PDA and PSS alternately. Chlorine tolerance, dye removal, salt rejection and flux experiments were done to investigate this strategy's efficiency. This sandwiched membrane resulted in better rejection (both salt and dye), good resistance to fouling, chlorine attack and excellent antibacterial performance. Thus the concept of using layer-by-layer self-assembly of polycations and polyanions onto a hierarchical chemically modified GO sandwiched PVDF membrane proved to be a productive strategy.

Methods
Materials and reagents
PVDF and PMMA was procured from commercial sources as mentioned in our earlier work [31]. GO was purchased from Log 9 (lateral dimension and thickness are 5 μm and 1–2 nm respectively). Acrylic acid (99%), dopamine hydrochloride, ammonium persulfate (APS), polystyrene with molecular weight ($M_n = 170,000$ and $M_w = 350,000$) were purchased from Sigma Aldrich. Sodium chloride, sodium hydroxide, magnesium nitrate, hexane, tetrahydrofuran, two propanols, ethanol, acetic acid, acetic anhydride, dichloromethane, sulphuric acid (98%) were supplied by local vendor. N-hydroxysuccinimide (NHS) (98%), methylenediamine dihydrochloride (98%) were provided by Sigma Aldrich and 1-(3-dimethyl aminopropyl)-3-ethyl carbodiimide hydrochloride (EDC) (98%) was supplied by TCI. No further purification of materials and chemicals were carried out before usage.

Membrane preparation
Fabrication of membranes using crystallization driven phase separation
A classical UCST (upper critical solution temperature) system i.e. blend of PVDF (semicrystalline polymer) and PMMA (amorphous) was choosen here to develop membranes with varying pore sizes. At high temperature (T > UCST), the phases are miscible and phase separates (T < UCST) upon cooling where one of the components (here PVDF) tend to crytsallize. The crystallization driven phase separation is dependent on the composition of blend (here PVDF ≥ 50%) as well as rate of cooling. [32] The PVDF content in the blends were varied from 50–70 wt%. A lab scale counter-rotating extruder was used to

melt process the blends at a speed of 60 rpm at 220 °C for about 20 min [33]. A laboratory hot press operated at 220 °C was used to hot press discs with a diameter of 60 mm and a thickness of nearly 80 μm. Selective etching of the PMMA phase was carried out using glacial acetic acid for seven days. The membranes which were derived from crystallization driven phase separation is shown in Fig. 1.

Fabrications of chemically crosslinked freestanding GO membrane

GO was chemically crosslinked using two steps process 1) activating of carboxyl groups using EDC and NHS coupling reagents 2) crosslinking with methylene diamine dihydrochloride. Firstly 30 mg of GO was added in 40 ml DI water and bath sonicated for 2 h. Then 100 mg EDC and 80 mg NHS were added simultaneously and stirred for four h followed by washing with DI water and dried at 50 °C for overnight. In the second step, activated GO was bath sonicated for one hour followed by 100 mg methylene diamine and stirred for 12 h. Finally, the chemically crosslinked freestanding GO was obtained by vacuum-assisted filtration. The reaction mechanism is depicted in the following Fig. 2.

Synthesis of Polydopamine (PDA)

PDA was synthesized by oxidant-induced polymerization technique as mentioned in the literature [34].

In brief, dopamine (4.0 g) as well as APS (the ratio is 5:3) were dissolved in DI water (400 ml). The polymeric reaction was carried at 70 ^{0}C for 84 h in the presence of an air environment. The product obtained after the given time was freeze-dried for one day under reduced pressure. The product was characterized using FTIR Spectroscopy (see figure S1).

Synthesis of Polystyrene sulfonate (PSS)

PSS is prepared from polystyrene by the method reported in the literature [35]. In brief,, dichloromethane (40.14 mL, 0.628 mol) and acetic anhydride (10.2 mL, 0.108 mol) are homogenized first under N_2 environment. 95–97% sulphuric acid (3.4 mL, 0.063 mol) was added carefully to the ice cooled mixture. A homogeneous and transparent solution was obtained on continuous stirring at room temperature. Then PS (1 g) was dissolved in 2.5 mL dichloromethane in two necked round bottom flask and acetyl sulfate solution (30 mL) was put in using a separating funnel. Then the mixture was heated at 60 ^{0}C under stirring for five h. The reaction was terminated by adding methanol (50 mL). The solution was dipped into boiling water (excess). It was further washed with sufficient water. After that, the product was filtered and dried under vacuum. The product was characterized using FTIR Spectroscopy (see figure S2).
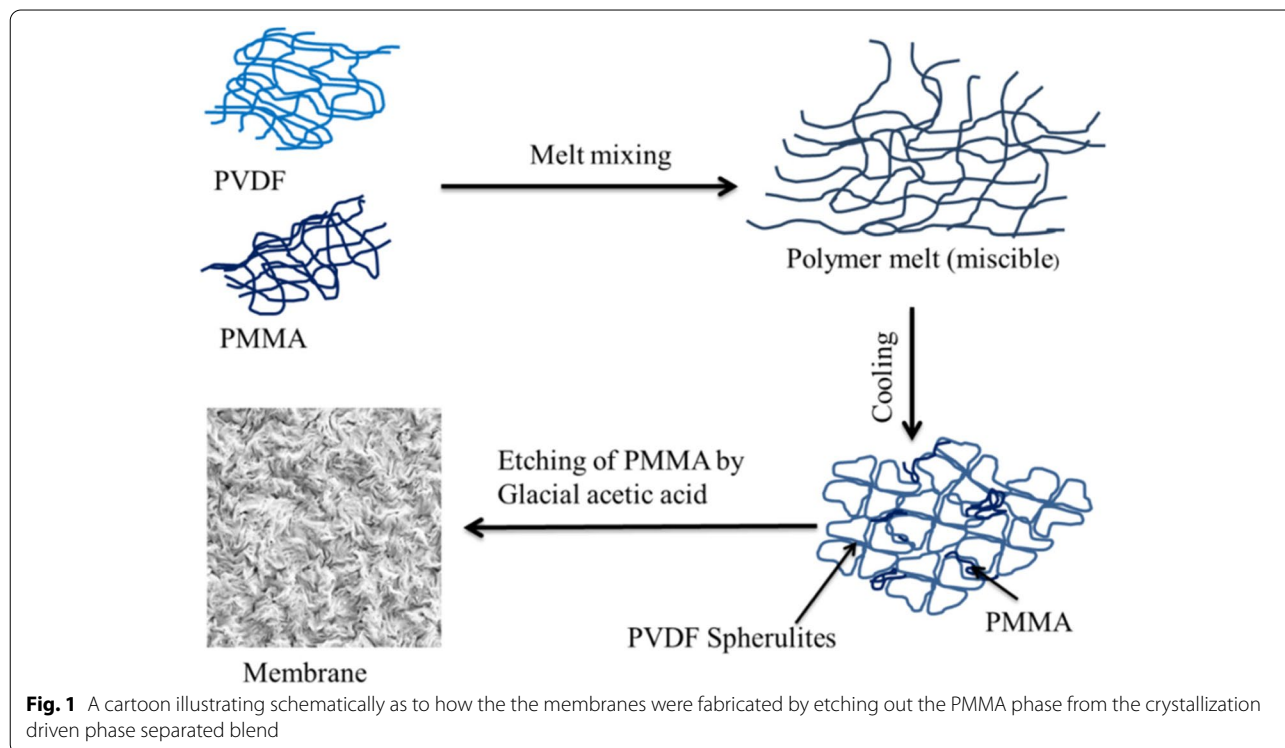

Fig. 1 A cartoon illustrating schematically as to how the the membranes were fabricated by etching out the PMMA phase from the crystallization driven phase separated blend
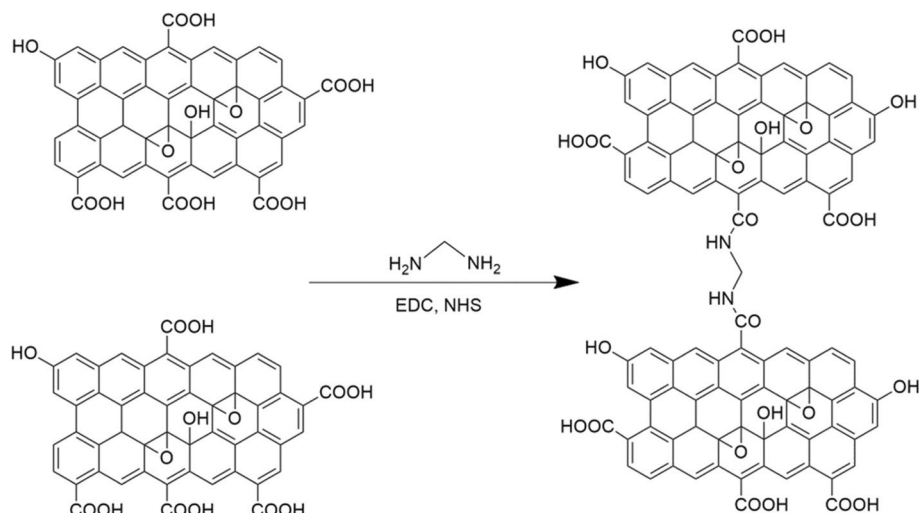
Fig. 2 Synthesis route of chemically crosslinked GO membrane

Self-assembly of polyelectrolytes supported on hierarchical membranes

The layer-by-layer polyelectrolytes were assembled on the pretreated PVDF membrane's surface (mentioned in supporting information figure S3) by depositing PDA (positive polyelectrolyte) and PSS (negative polyelectrolyte) alternatively. Firstly, only PDA aqueous solution (0.01 g/ml) was coated onto the PVDF membrane's surface, followed by vacuum drying at 50 °C for overnight. Then PSS organic solution (0.01 g/ml) and PDA aqueous solution were coated alternatively ten times. And finally, the composite membrane was vacuum dried at room temperature overnight. Figure 3 shows the scheme for the fabrication of polyelectrolytes modified chemically crosslinked GO sandwiched composite membranes

(referred to as PSS-PDA-crosslinked GO membrane hereafter).

Thus PSS-PDA-cross-linked GO membrane was fabricated first by stitching crosslinked freestanding GO membrane in between the 50/50 and 60/40 membranes self-assembly of polycations and polyanions was done on the active 50/50 surface. Table 1 briefly describes the various membranes that are prepared in this study.

Characterization of the membranes

The membranes and polyelectrolytes were analyzed using FTIR in the mid-IR range, i.e. (4000 cm^{-1} to 650 cm^{-1}) on a Perkin Elmer Frontier. The micrographs of the surface and cross-section were recorded using a SEM. The cross-sections of samples were made by dipping in liquid
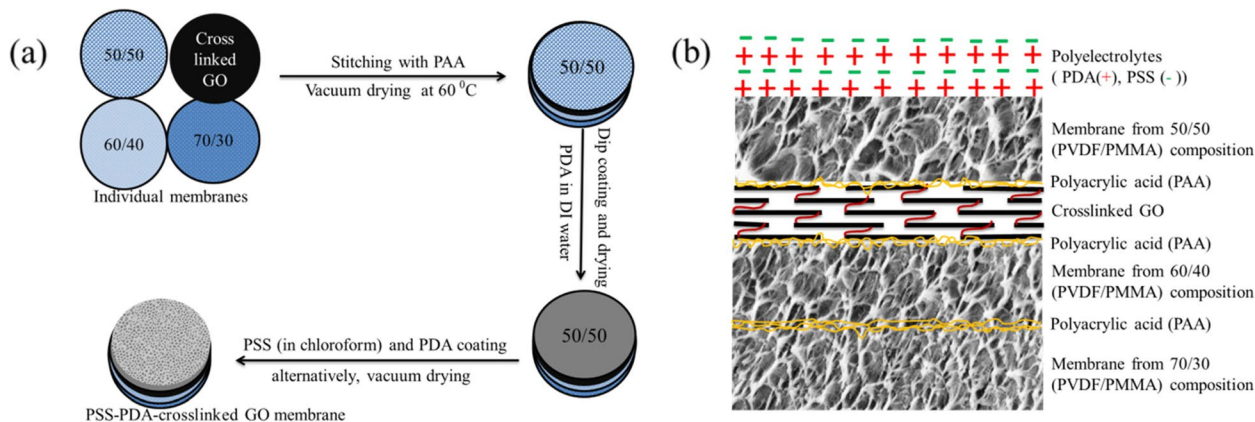

Fig. 3 A cartoon illustrating schematically (**a**) fabrication of PSS-PDA-crosslinked GO membrane (**b**) how different layers are stacked together in PSS-PDA-crosslinked GO membrane

Table 1 Brief description about all the prepared membranes

Membranes	Preparation method	Characteristics
PVDF/PMMA (These are named as 50/50, 60/40 and 70/30 based on composition in blend)	These membranes are prepared from the blend of PVDF and PMMA by etching out the PMMA phase	These are microporous membranes with pore sizes 200, 140, 80 nm for 50/50, 60/40 and 70/30 respectively
Control membrane	Membranes derived from 50/50, 60/40 and 70/30 blends stitched with PAA such that 50/50 is the active surface	This hierarchical membrane offers gradient in morphology
GO membrane	It is prepared via vacuum assisted filtration on the commercial PVDF support	This membrane is a freestanding membrane in which GO flakes are nicely deposited on PVDF support
Crosslinked GO membrane	Same as GO membrane	Here GO falkes are chemically stitched which arrests the swelling of GO under aqueous environment
GO modified membrane	Freestanding GO membrane was stitched between 50/50 and 60/40 membrane	Here GO helps to improve the performance of the control membrane
PSS-PDA membrane	This membrane was prepared by depositing PDA and PSS electrolytes alternatively on the surface of pretreated control membrane	The layer by layer assembly of polyelectrolytes on the top surface of the membrane helps to improve in separation and fouling resistance
PSS-PDA-crosslinked GO membrane	Freestanding crosslinked GO membrane was stitched in between 50/50 and 60/40 membrane followed by deposition of PDA and PSS electrolytes alternatively	The layer by layer assembly of polyelectrolytes on the top surface of the membrane and the position of crosslinked GO membrane help to synergize the membranes performance

nitrogen followed by cryo fractured and fixed them to the SEM stub. Water was used as a solvent to measure the contact angle of the hydrophilic membranes. The freestanding GO was identified using XRD. The modified membrane's surface charge was estimated at pH 7 using SurPASS 3 by Anton Paar as mentioned in our previous work [31].

Application of membranes
Permeation analysis and dynamic antifouling studies:

a) Water flux

Flux experiment was performed by using a in-build cross flow setup. Membranes having 47 mm diameter were compacted in the cross-flow module setup at a pressure of 0.21 MPa for nearly half an hour. Subsequently, the data was collected by setting the transmembrane pressure at different values ranging from 0.21 to 0.51 MPa. Each reading was repeated three times to check its reproducibility and was compared with the control membrane.

b) *Dye rejection studies*

MB and CR were used as the model dyes and were hence used to demonstrate the dye rejection abilities of the fabricated membranes. DI water was used to prepare 100 ppm dye solutions. A transmembrane pressure of 0.41 MPa was applied in the cross-flow setup for studying the dye removal capabilities. UV vis Spectrophotometry was used to check the concentration of the permeate solution and % rejection was calculated by the formula:

$$\% \text{ Rejection} = [1 - (C_{ps}/C_{fs})] * 100 \tag{1}$$

where C_{ps}= permeate concentration in ppm and C_{fs} = feed concentration in ppm.

c) Salt rejection studies

The sample draw solutions of 2000 ppm was prepared in DI water using monovalent as well as a divalent salt, i.e., NaCl and $Mg(NO_3)_2$ separately. FO setup was used to study the rejection performance. For the abovementioned experiments, water (20 ppm) was taken in the feed. The TDS meter was used to monitor the concentration of both feed and draw solution at regular intervals. Equation 2 was utilized to determine the rejection efficiency.

$$\% \text{ Rejection} = [1 - ((C_{ff} - C_{if})/C_{id})] * 100 \tag{2}$$

where C_{ff} and C_{if} are the final and initial concentration of feed in ppm respectively and C_{id}= initial concentration of draw in ppm.

d) Dynamic antifouling studies

BSA was used as the model foulant to investigate the dynamic antifouling properties. Keeping at per with the literature [36], a 1 g/L solution of BSA was prepared in DI water. Subsequently, three cycles of flux operation were performed. At first, J_w was recorded, which is the pure water flux. Following this, the same experiment was repeated using the BSA solution as the feed and J_B was recorded. Finally, backflushing with 1X phosphate-buffered saline (PBS) was carried out for 30 min and once again the pure water flux, i.e., J_P, was recorded. The irreversible flux decline

ratio (IFR), relative fouled flux ratio (RFR) and flux recovery ratio (FRR), were used to determine the antifouling properties of these membranes. If FRR is high, then the membrane has a superior tendency to resist fouling attacks. The RFR, IFR and FRR were estimated by putting the flux value on the given equations.

$$FRR(\%) = \frac{J_P}{J_W} \times 100 \qquad (3)$$

$$IFR(\%) = 100 - FRR \qquad (4)$$

$$RFR(\%) = \frac{J_B}{J_W} \times 100 \qquad (5)$$

Bacteriological assessment
The bacteriological studies were performed with model bacterial strains which included gram-negative *E. coli* ATCC25922 and gram-positive S. aureus ATCC25923. The detail of the method was shown in earlier work. [37]

Resistance to chlorine
Resistance to chlorine was generally measured by the difference or variance in salt rejection before and after exposure in sodium hypochlorite solution. Smaller the declination in salt rejection after chlorine treatment better is the resistance to chlorine. At first sodium hypochlorite solutions of concentration of 2000 ppm, 4000 ppm, 6000 ppm, 8000 ppm, 10,000 ppm having pH 10 were prepared. The PSS-crosslinked GO membrane was exposed to 2000–10,000 ppm h in solutions followed by washing nicely with sufficient pure water. The rejection of this membrane on exposing to 2000–10,000 ppm chlorine solutions every hour was recorded in the same way using FO experiment.

Results and discussion
Micrographs showing the surface as well as cross-sectional images of the membranes
FESEM was used to observe and analyze the fabricated membranes' surface as well as cross-sectional morphology. Results indicated the presence of spherulitic morphology for all the etched blends. The corresponding surface SEM images obtained for 50/50, 60/40 and 70/30, PVDF/PMMA etched blends are shown in Fig. 4 (a, b, e, f, i, j). The spherulitic size was observed to be smaller with increasing PMMA concentration. The corresponding cross-sectional morphologies are illustrated also in Fig. 4 (c, d, g, h, k, l). An unimpeded water flow was an outcome of the spongy, porous morphology. 200, 140, and 80 nm, respectively, are the average pore sizes of the
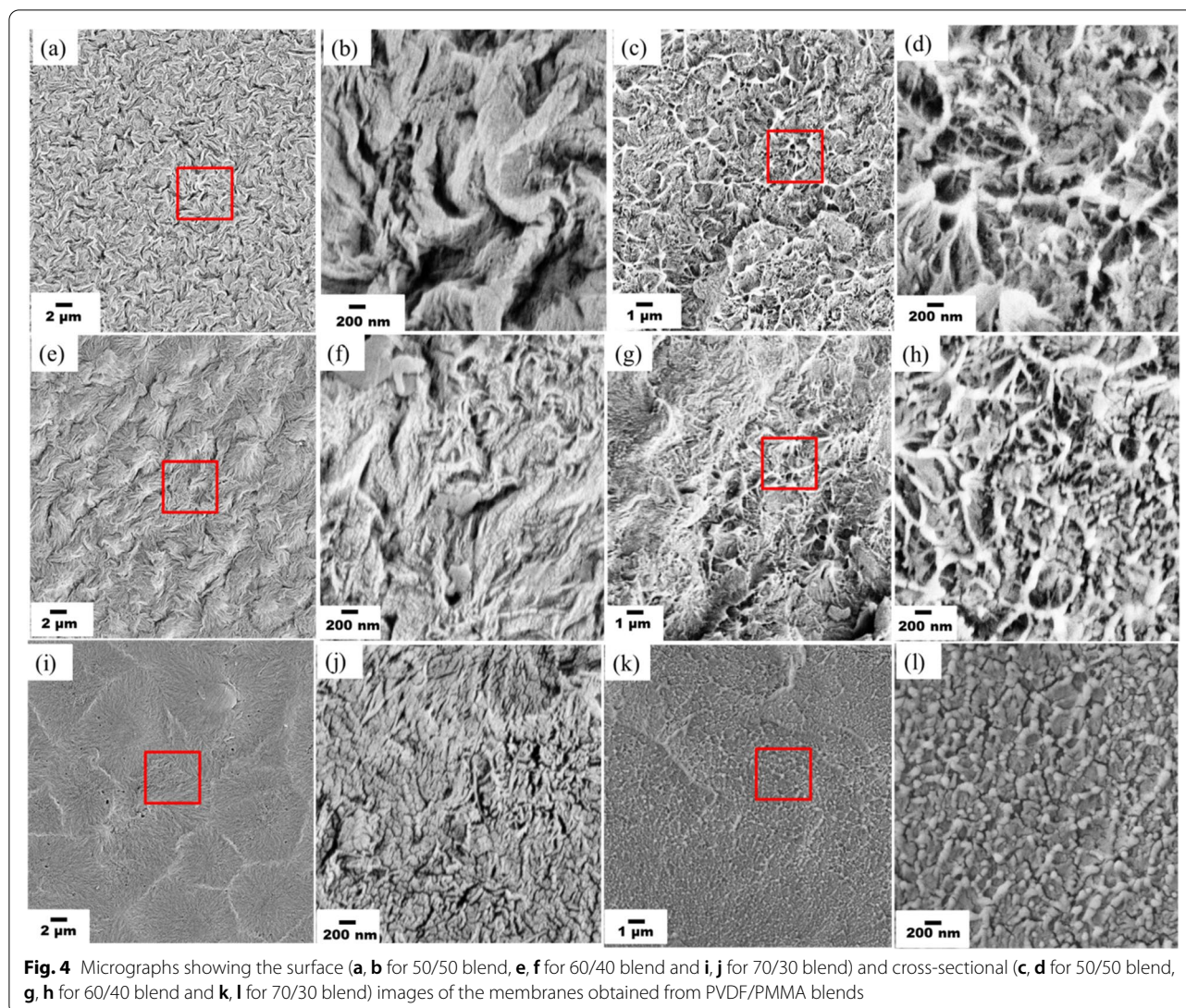
50/50, 60/40, and 70/30 blend membranes. Thus, it was corroborated from the SEM micrographs that varying compositions played a significant role in controlling the pore sizes.

Rejection performance and pure water flux of the fabricated membranes
The water flux of all fabricated membranes were calculated at a transmembrane pressure 0.413 MPa. The 50/50, 60/40 and 70/30 membranes showed a permeate flux of 2000 ± 100 Lm-2 h-1, 1660 ± 80 Lm-2 h-1, and 970 ± 40 Lm-2 h-1, respectively. Due to the membranes' microporous nature, their dye rejection was not impressive, although each membrane individually showcased higher water flux than commercially available nanofiltration membranes. Hence, a unique approach by rationally stacking various membranes for better separation was adopted here. To accomplish this, polyacrylic acid was used to stitch the three fabricated membranes, which was referred to as the control sample. This was subsequently sandwiched with chemically crosslinked freestanding GO and modified the membrane's surface with layer by layer assembly of polyelectrolytes (referred to as PSS-PDA-crosslinked GO membrane) for improved dye, salt rejection, chlorine tolerance and antibacterial performance discussed as in Fig. 3.

Characterization of freestanding GO membrane by XRD
Structural properties of freestanding GO and chemically crosslinked freestanding GO in dry and wet conditions (immersed in DI water for 24 h) were analyzed by Xpert Pro using Cu Kα as a source. All the samples were scanned from 5° to 80° with a step size of 0.049°. The XRD pattern of all these freestanding GO is shown in Fig. 5. A prominent peak at $2\theta = 10.4°$ (interlayer or d-spacing of 8.56 A°) is observed which corresponds to the oxidized graphitic peak for pristine freestanding GO. The shifting of peak to higher 2θ (from 10.4° to 13.24°) for chemically crosslinked freestanding GO clearly shows the interlayer spacing of 6.67 A°. From this data, it can be assured that the amine functional groups of methylene diamine reacted with functionalities (GO). These are interconnected within sub-nano-channels of GO, thus reducing d- spacing (from 8.56 A° to 6.67 A°). It is further analyzed that the peak was shifted to lower 2θ value from 10.4° to 7.15° (interlayer spacing from 8.56 A° to 12.33 A°) for pristine GO in wet condition after immersing it in water for 24 h. In contrast, there is almost no shifting in the peak position for chemically crosslinked GO under the same immersing condition. From these data, it can be suggested that the free passage of water molecules within the layers of pristine GO enlarged the interlayer spacing.

Fig. 4 Micrographs showing the surface (**a**, **b** for 50/50 blend, **e**, **f** for 60/40 blend and **i**, **j** for 70/30 blend) and cross-sectional (**c**, **d** for 50/50 blend, **g**, **h** for 60/40 blend and **k**, **l** for 70/30 blend) images of the membranes obtained from PVDF/PMMA blends

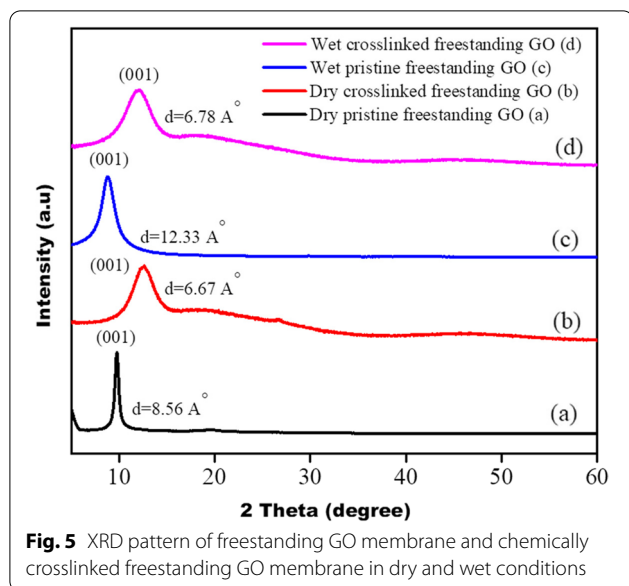In contrast, chemically crosslinked GO did not swell, manifested from constant d-spacing of near about 6.7 Å.

Spectroscopic evidence

The chemically crosslinked GO was characterized by FTIR spectrum as shown in Fig. 6A. It is observed that after crosslinking the GO sheets with methylene diamine, the intensity of –C=O stretching of carboxyl groups was significantly reduced. Moreover, the appearance of -CH2 stretching peak at near about 2964 cm-1 and –C-N stretching peak at near about 1247 cm^{-1} suggests the confirmation of chemically interlocking GO sheets that reduce the interlayer spacing as confirmed from XRD analysis (Fig. 5). The polyelectrolytes modification onto the membrane's surface was also corroborated by FTIR spectrum (Fig. 6B). The stretching of the sulfonate group peak at near about 1080 cm^{-1} confirms the polystyrene

sulfonate layer onto the membrane's surface. Moreover, the appearance of –NH stretching in the range 3150 to 3300 cm-1 also suggests the assembly of polydopamine onto the surface of the membrane.

Micrographs showing the surface as well as cross-sectional images of the amended membranes

For gauging the membrane's surface characteristics and ascertain the self-assembly of the polyelectrolytes, forming the active surface, SEM was performed. The control membrane's surface morphology is depicted in Fig. 7(a). From Fig. 7(b) and(c), micrographs showing the surface and cross-sectional images of the membranes modified with polyelectrolytes can be observed. It can be rightly concluded from the cross-sectional micrographs and the EDX analysis that there has been a deposition of

Fig. 5 XRD pattern of freestanding GO membrane and chemically crosslinked freestanding GO membrane in dry and wet conditions

self-assembled polyelectrolytes (thickness ranging from 7–9 μm).

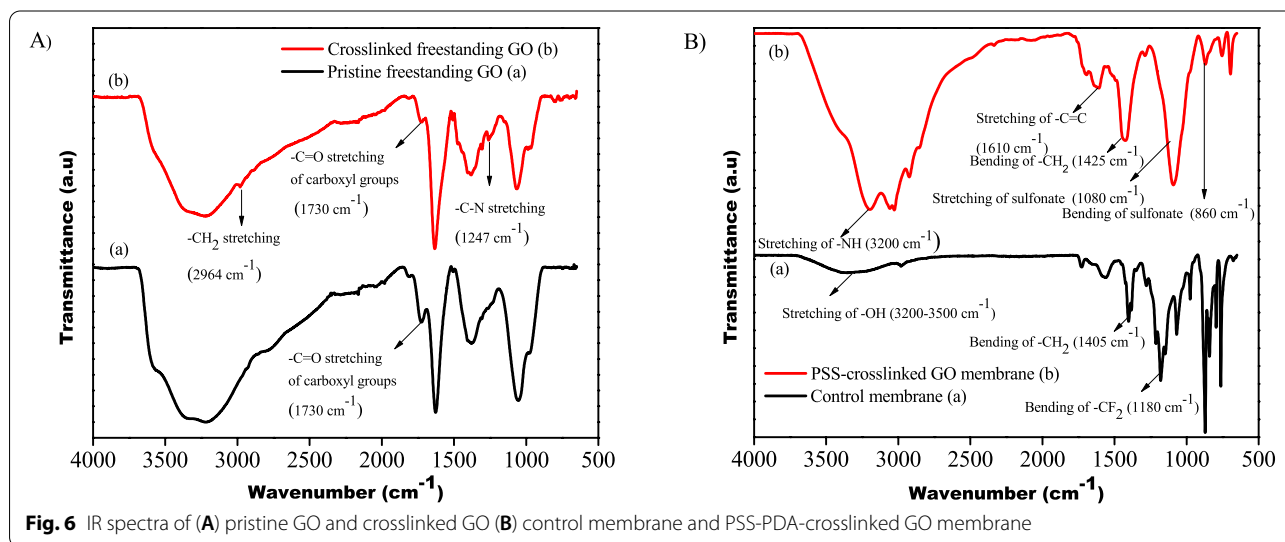### Contact angle and zeta potential of PSS-PDA-crosslinked GO and control membranes

The potential present at the shear plane in between the surface and solution is known as Zeta potential. Steaming potential from Helmholtz-Smoluchowski Equation [38] was used to determine the control and modified membranes' Zeta potential. SurPASS 3 was utilized to determine the membranes' surface charge or zeta potential by the procedure mentioned in our previous work [31]. It was seen that the PSS-PDA-cross-linked GO

membrane demonstrated a significantly less negative zeta potential of -13 mV as compared to the control membrane (-26 mV), as depicted in (Fig. 8a). Reason being the reduction of negative charge of PSS by the influence of PDA and/or as the PSS layer is highly porous so there is a possibility of PDA coating to influence in the surface charge, which was also seen in FTIR and is confirmed by surface SEM EDX analysis.

An important technique utilized to determine hydrophilicity is the water contact angle. Static contact angle was determined for each membrane to ascertain their hydrophilicity. Lower contact angle is related to higher hydrophilicity, which assures the membrane's better affinity towards water. $86 \pm 3°$ was contact angle of prepared control membrane and $49 \pm 2°$ was that of the PSS-PDA-crosslinked GO membrane (Fig. 8b). A sudden and prompt reduction in contact angle signifies the presence of a hydrophilic surface in the PSS-PDA-cross-linked GO membrane. The surface charges induced by the by self-assembly of oppositely charged polyelectrolytes is the reason behind the significant decline in contact angle.

Pure water flux

The experiments were performed at 0.423 MPa for the control membranes, GO modified membranes, and crosslinked GO modified membranes. The flux values obtained were 150 ± 10 Lm-2 h-1 and 145 ± 8 Lm-2 h-1, 130 ± 6 Lm-2 h-1, respectively. Polyelectrolytes modified stacked membrane (referred as PSS-PDA membrane hereafter) and PSS-PDA-crosslinked GO membrane shows water flux 159 ± 12 Lm-2 h-1, 137 ± 7 Lm-2 h-1, respectively (Fig. 9a). It is observed that flux is decreased in GO modified membrane compared to control membrane due to tortuous paths and
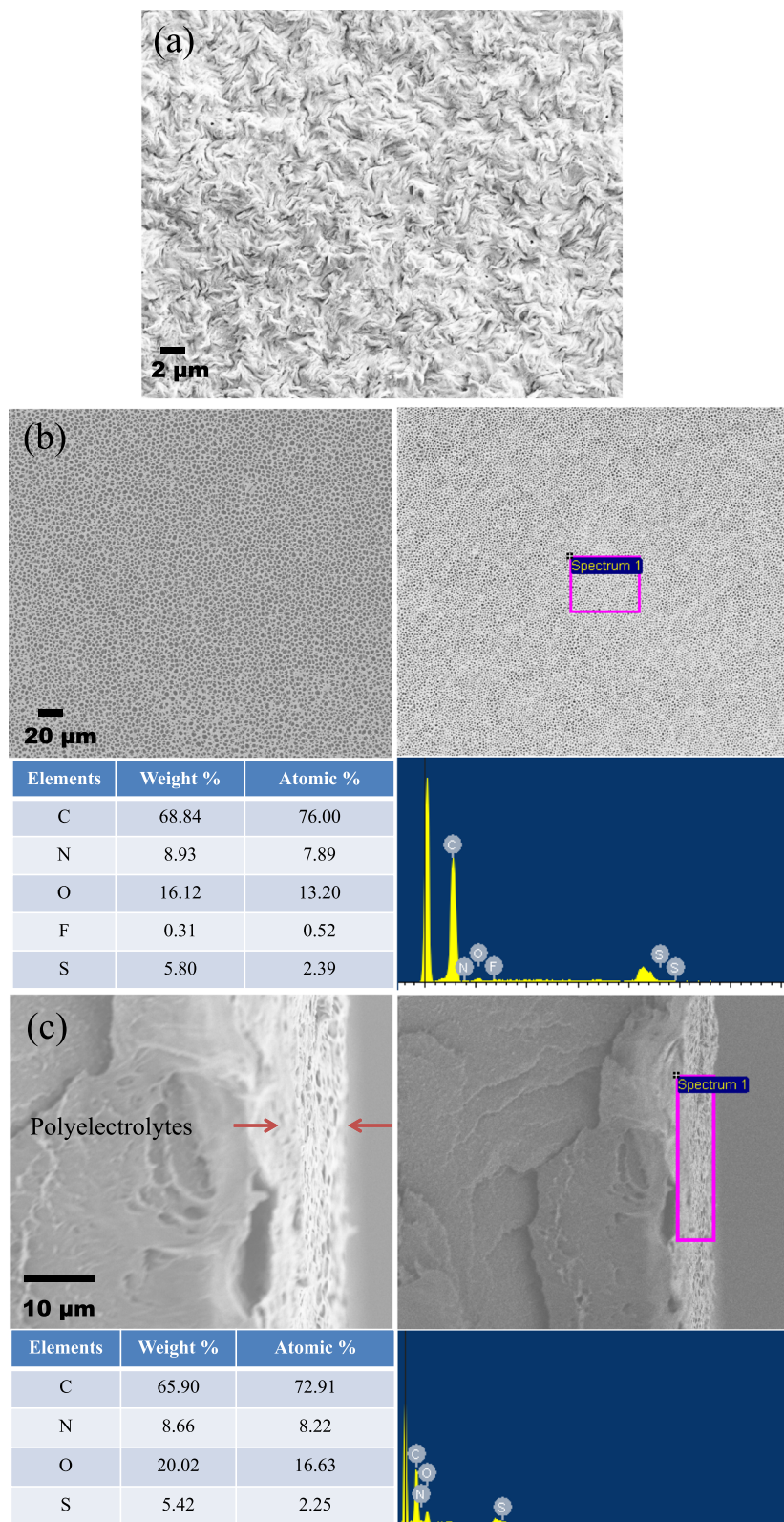

Fig. 6 IR spectra of (**A**) pristine GO and crosslinked GO (**B**) control membrane and PSS-PDA-crosslinked GO membrane

Elements	Weight %	Atomic %
C	68.84	76.00
N	8.93	7.89
O	16.12	13.20
F	0.31	0.52
S	5.80	2.39

Elements	Weight %	Atomic %
C	65.90	72.91
N	8.66	8.22
O	20.02	16.63
S	5.42	2.25

Fig. 7 Micrographs showing the surface images of control membrane (**a**) polyelectrolytes modified membrane along with its EDX (**b**) and the cross-section image of polyelectrolytes modified membrane along with its EDX (**c**)

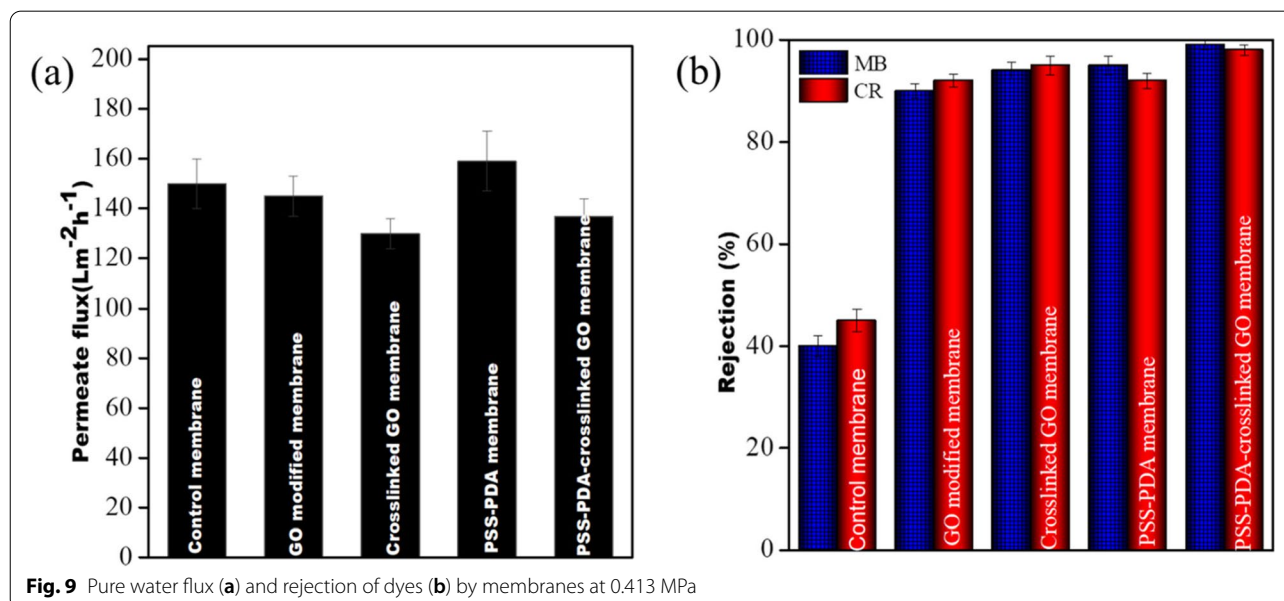**Fig. 8** Control and PSS-PDA-crosslinked GO membranes' Zeta potential (**a**) and Contact angle (**b**)
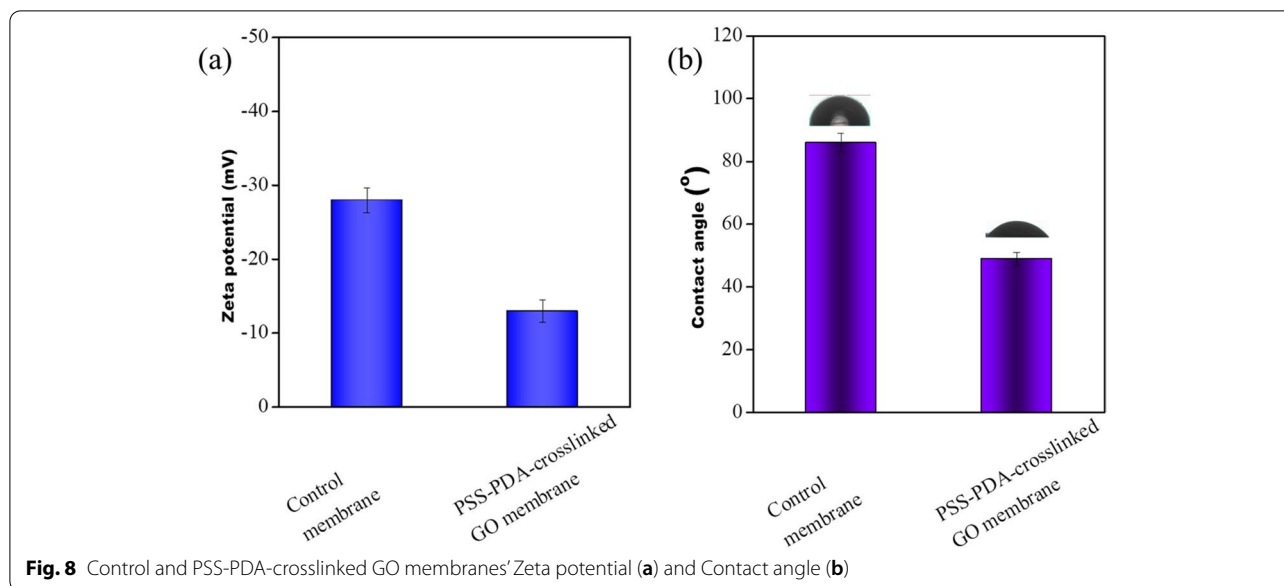
less interlayer spacing, which easily restricts water flow. For chemically crosslinked GO membrane, the interlayer spacing is reduced as confirmed by XRD (Fig. 5) that the flux significantly decreased to 130 LMH. In the PSS-PDA membrane, significant flux improvement is observed because of charged polyelectrolytes assembly.

Dye removal studies

The dye removing capacities were determined for all the modified membranes in intensified conditions. 100 ppm feed of Congo red (CR) and methylene blue (MB were used as the model dye foulants. Results indicated that all the modified membranes could efficiently reject more than 90% of both the dyes @ 0.423 MPa. An outstanding performance was obtained in the case of PSS-PDA-crosslinked GO membrane, it was more than 99% and 98% for cationic dye and anionic dye, respectively (Fig. 9b). The control membrane shows rejection near about 50%. Adsorption of the cationic dyes and repulsion of the anionic ones from the membrane surface is probably the primary reason behind the high dye rejection efficiency of the PSS-PDA-crosslinked GO membrane.

Fig. 9 Pure water flux (**a**) and rejection of dyes (**b**) by membranes at 0.413 MPa

Its converse can also be accurate because of electrostatic interaction with polyelectrolytes as well as pore-based sieving due to crosslinked non-swellable GO.

Antifouling studies in dynamic conditions

The control and PSS-PDA-crosslinked GO membrane's antifouling characteristics were estimated using RFR, IFR, and FRR as represented in (Fig. 10a). The PSS-PDA-crosslinked GO membrane exhibited a FRR value greater than 90%, while it was just 60% for the control one. The surface charge brought by the assembly of the polycations and polyanions is the primary reason behind the high FRR values of the PSS-PDA-crosslinked GO membrane.
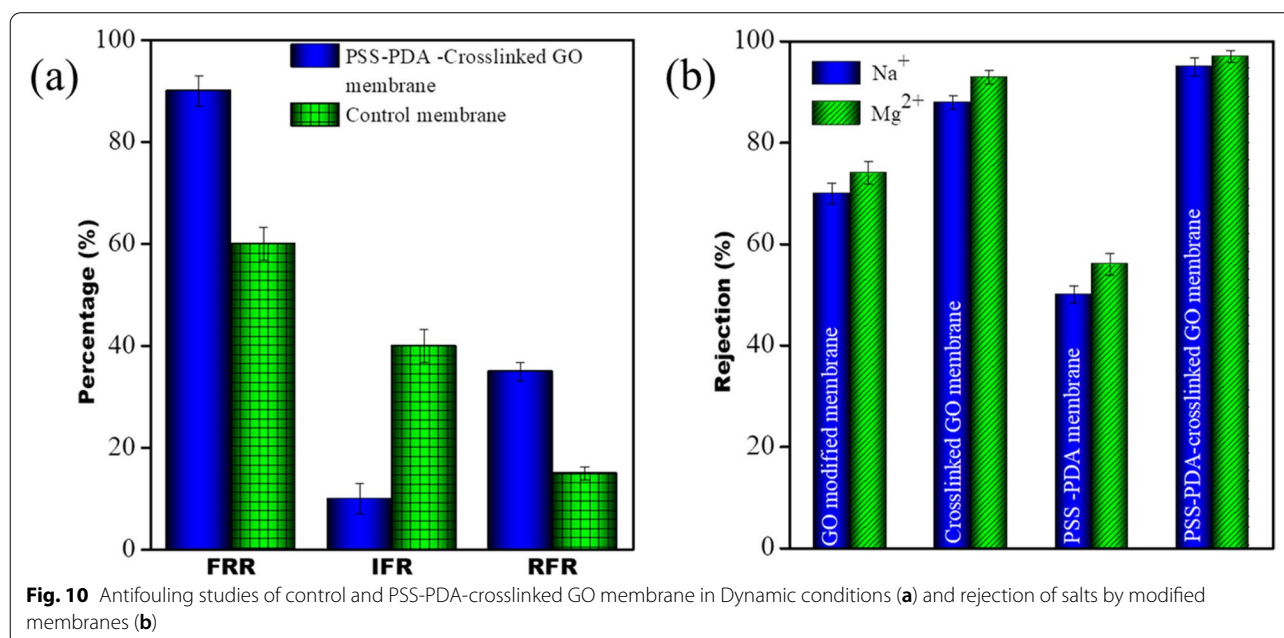
FO assisted rejection studies

Pressure enhanced FO was used to study the sieving performances of all the modified membranes at 0.068 MPa [39]. NaCl solution of 2000 ppm and another $Mg(NO_3)_2$ solution of 2000 ppm were taken separately as draw solution. Water (20 ppm) was taken in the feed. Concentrations of both feed and draw solutions were measured in each specific interval. Rejection for GO modified membrane, crosslinked GO membrane, PSS-PDA membrane, and PSS-PDA-crosslinked GO membrane were more than 70%, 90%, 50%, and 95%, respectively for both monovalent and divalent ion (Fig. 10b). The PSS-PDA-crosslinked GO membrane's highest efficiency is because of electrostatic interaction in addition to the pore-based sieving. The rejection in PSS-PDA-crosslinked GO membrane is quite significant (> 5%) than only crosslinked GO membrane due to the presence of polyelectrolytes on the surface. Interestingly, the rejection was significantly higher (70%) in the case of GO modified membrane as compared to only PSS-PDA membrane (50%). This is due to synergistc combination of pore and charge-based separation in the case of only GO and only charge-based in the case of later. The control membrane (without GO and/or PSS-PDA) showed < 30% rejection owing to bigger pores.

Resistance to chlorine

To investigate the performance, the PSS-PDA-crosslinked GO membrane was exposed to 2000–10,000 ppm solutions for an hour, and then the membrane was washed nicely with sufficient pure water. The salt rejection of this membrane on exposing to 2000–10,000 ppm chlorine solutions every hour was recorded in the same way using FO experiment. It is observed that there is a no declination of rejection even on exposing to NaOCl solution up to 4000 ppm and there is a slight decrease near about 2% on exposure in 6000 ppm solution. The membrane rejection efficiency was decreased significantly near about 7% on exposure to 10,000 ppm solution. The resistance towards chlorine exposure of this membrane can explain that free chlorine may be entrapped into primary or secondary amine of polydopamine, which helps the crosslinked GO attain structural stability. When the concentration is more, there is a sufficient amount of free chlorine, which may attract the amide linkage of crosslinked GO, and therefore, the bond may become too weakened to suppress the passage of salt ions. So the rejection efficiency becomes less on exposure in higher
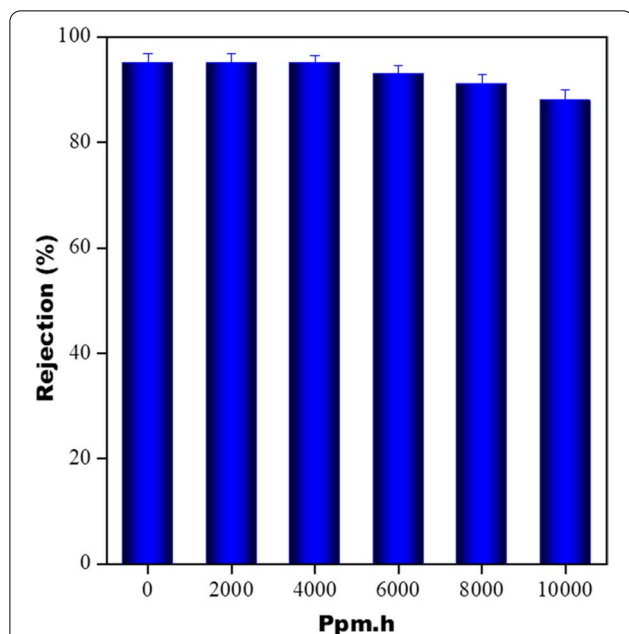

Fig. 10 Antifouling studies of control and PSS-PDA-crosslinked GO membrane in Dynamic conditions (**a**) and rejection of salts by modified membranes (**b**)

Fig. 11 Rejection performance (monovalent ion) of PSS-PDA-crosslinked membrane on chlorine exposure

concentrated NaOCl solution. Therefore the PSS-PDA-crosslinked GO membrane shows excellent chlorine tolerance property. The rejection performance of the PSS-PDA-cross-linked GO membrane after chlorine exposure is shown in Fig. 11.

Antibacterial performance

A standard plate count method was performed to assess the PSS-PDA-crosslinked GO membrane's antibacterial efficiency. As seen from figure S4 (a-d), it is observed that for the incubation period of 2 h, the colonies were reduced by threefold for both strains. After incubation, membranes were fixed with 4% formaldehyde and the morphologies of the bacterial cells attached on the membrane's surface were perceived via. FE-SEM. It is observed that the cell integrity of both bacteria was severely damaged. In contrast, the cells adhered to the control membrane remained intact and formed a noticeable biofilm (Fig. 12a-d). These results suggest that the PSS-PDA-crosslinked GO modified membrane are antimicrobial in nature manifested from the results against both the bacterial strains. The solid electrostatic interaction of
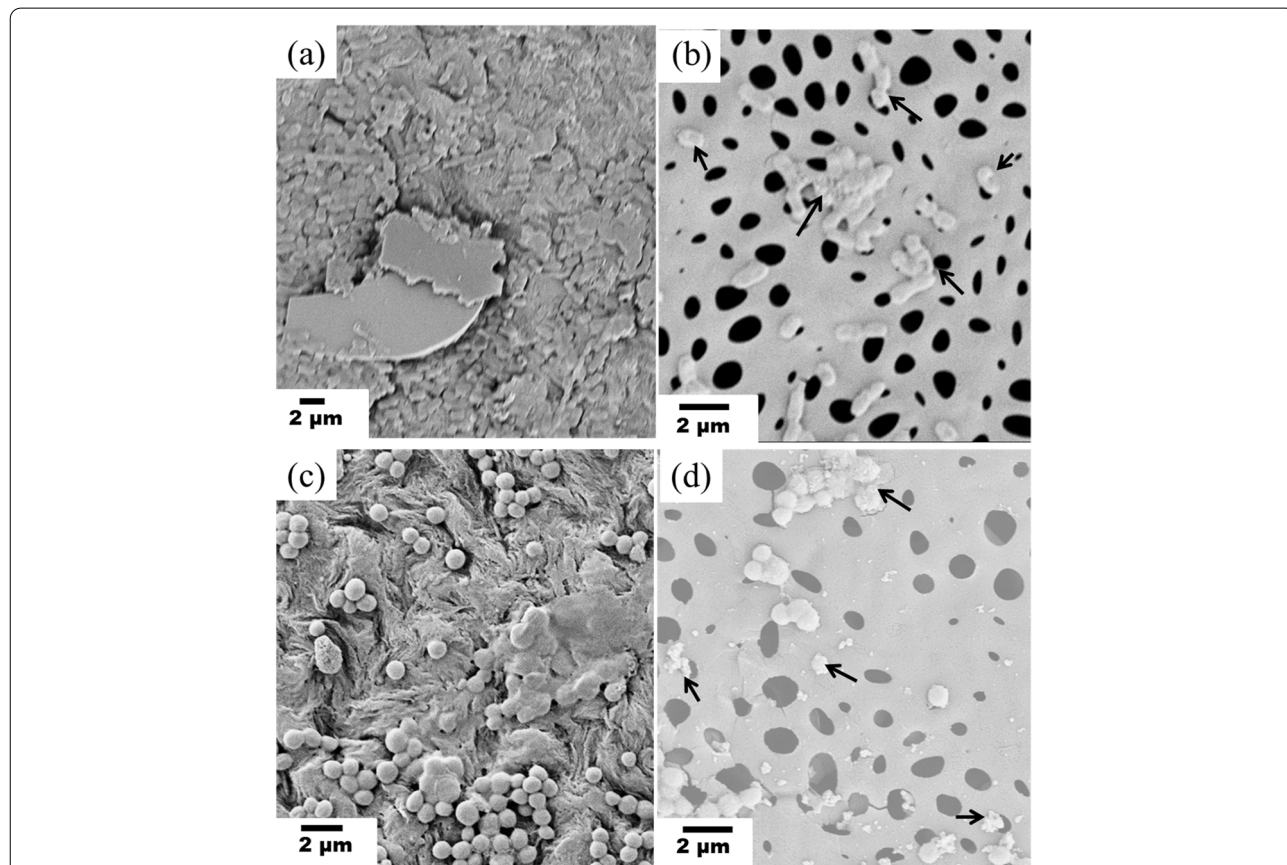

Fig. 12 SEM image of control membrane (**a**, **c**) and PSS-PDA- crosslinked GO membrane (**b**, **d**) on incubation for 2 h with E. coli and S. aureus respectively. The arrow marks show destruction of cells

polyelectrolytes with the bacterial cell membrane may damage the cell wall.

Discussion

In this work, a novel composite membrane was fabricated by 'layer-by-layer self-assembly of poly-dopamine (Polycation) and polystyrene sulfonate (Polyanion) supported on a highly chemically crosslinked graphene oxide (GO) sandwiched PVDF membrane. This membrane shows outstanding performance in sieving ions, chlorine tolerability, antifouling, and antibacterial performance. The exceptional performance was due to the vital role of both the self-assembly of polyelectrolytes and chemically crosslinked GO membrane as shown in the Fig. 13.

The modified membrane also shows significant flux improvement compared to the control membrane because of enhancement of hydrophilic surfaces imparted by charged polyelectrolytes assembly. The charge surface resists the fouling attack by repelling the negative charged BSA used as a model foulant. Adsorption of the cationic dyes and repulsion of the anionic ones from the membrane surface is probably the primary reason behind the outstanding dye rejection efficiency of the PSS-PDA-crosslinked GO membrane. Its converse can also be accurate because of electrostatic interaction with polyelectrolytes as well as pore-based separations due to crosslinked non-swellable GO. The PSS-PDA-crosslinked GO membrane's outstanding rejection is because of electrostatic interaction in addition to the

pore-based sieving. The monovalent or divalent ions are electrostatically bound to the negatively charged surface of the membrane. The ions passed through the polyelectrolyte layer are finally sieved by the crosslinked GO membrane (minimal interlayer spacing as supported from XRD, Fig. 5), contributing to the less reverse salt flux. In the case of only PSS-PDA membrane, the rejection of ions are not significant as ions are rejected by polyelectrolytes. The rejection is more in the case of GO modified membrane due to small interlayer spacing whereas, the rejection was quite significant in the case of crosslinked GO modified membrane as the swelling (of GO) is arrested due to crosslinking. Interestingly, a combination of crosslinked GO and polyelectrolyte synergies the sieving performance in PSS-PDA crosslinked GO membrane. The resistance towards chlorine exposure of this membrane can explain that free chlorine may be entrapped into primary or secondary amine of polydopamine, which helps the crosslinked GO membrane attain structural stability. The solid electrostatic interaction of polyelectrolytes with the bacterial cell membrane may damage the cell wall, manifesting the membrane as an effective antimicrobial. Thus the PSS-PDA-crosslinked GO membrane show robust performance in terms of separation as well as resistance to fouling. In this context, various reserachers have reported GO-based membranes with or without modification however, our approach can be well appreciated from the rejection performance. For instance, Yang et al. [40] prepared rGO
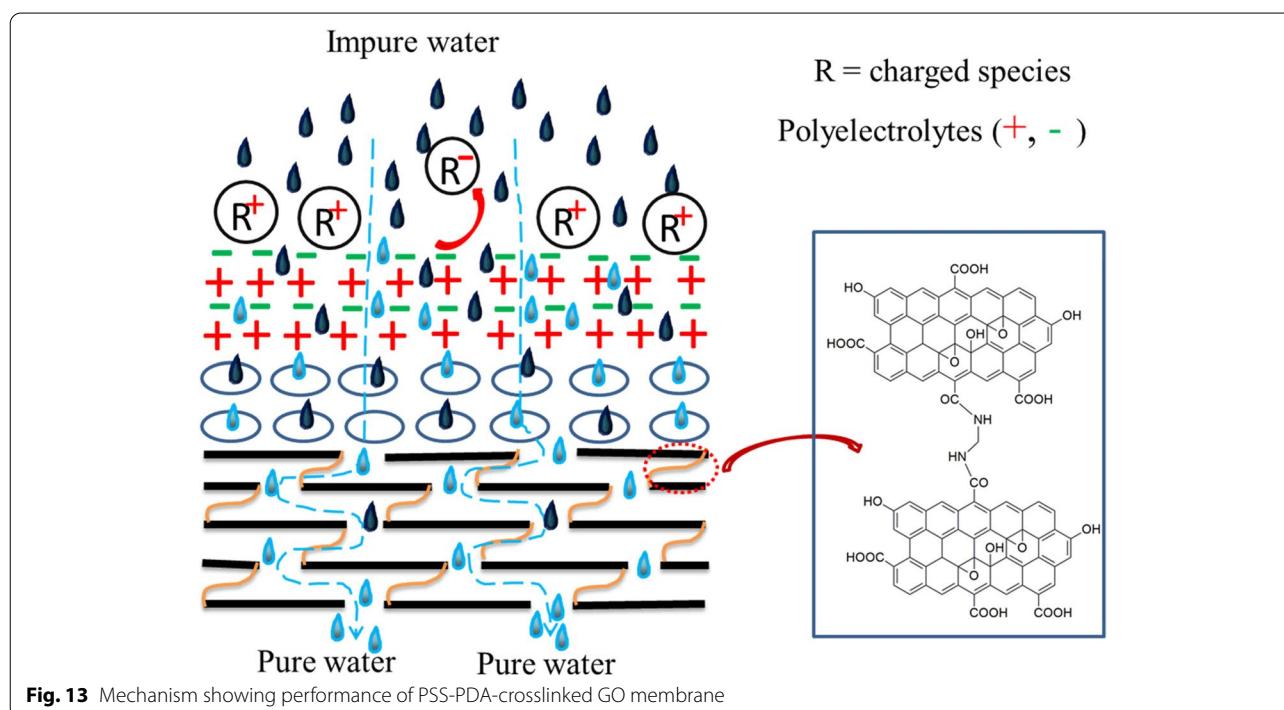

Fig. 13 Mechanism showing performance of PSS-PDA-crosslinked GO membrane

Table 2 Comparison studies of rejection of some FO membranes published in the literature

Membranes	Feed solution	Draw solution	Water flux (LMH)	Rejection rate	References
PSS-PDA crosslinked GO	DI water	2000 ppm NaCl and Mg (NO$_3$)$_2$ solution	32	95% and 97%	this work
GO-(SiO$_3$)$_X$	DI water	1.5 M NaCl solution	30	88%	[42]
GO/ Poly (NIPAM-MBA)	DI water	1 M NaCl solution	25.8	99.9%	[41]
		50 mM NaCl		53% 97%	
PSS-PAH	DI water	MgSO$_4$ MgCl$_2$ Na$_2$SO$_4$	20	98% 86%	[43]
G-GQD	DI water	2000 ppm Na$_2$SO$_4$ solution	27	97%	[39]
pDA coated rGO	DI water	0.6 M NaCl solution	36.6	92%	[40]

laminates on a mixed cellulose ester membrane and was coated with polydopamine. The rejection is ca. 92%. In this approach they did not attempt to stitch the GO layers. Kim et al. [41] prepared GO composite crosslinked with polymer network which shows good rejection performance. Jia et al. [42] synthesized GO composite membrane using silanol deposited by layer-by-layer self assembly method. Reurink et al. [43] prepared polyelectrolyte multilayer membranes by layer-by-layer assembly of polyelectrolytes on to a tight hollow fibre membrane and they evaluated salt rejection performance using different draw solutions. Padmavathy et al. [39] crosslinked GO with graphene oxide quantum dots (GQD) and used in both FO mode (for salt rejection) and RO mode (for dye rejections). In this work, we crosslinked GO chemically using monomethylene diamine and were able to fabricate a freestanding membrane which was sandwiched between the two polymer membranes. We deposited polyelectrolytes by layer-by-layer method on the active surface of the sandwich membrane. This membrane has been used both in FO and RO mode, and showed excellent rejection performance. A comparison study showing the rejection performance of various GO-based membrane is illustrated in Table 2.

Conclusion

In this work, membranes with varying pores were obtained by vaying the composition in blend (PVDF/PMMA), and etching out the PMMA phase. We tuned the d -spacing and enhanced the dimensional stability of GO by chemically crosslinking with methylene diamine and make it a freestanding membrane that is sandwiched in between membranes to enhance rejection efficiency. The active surface was further modified with an assembly of oppositely charged polyelectrolytes to improve better rejection performance. Thus the modified membrane showed excellent salt rejection (about 95% and 97% for monovalent and divalent ions

respectively) and outstanding dyes rejection (almost 100% for both cationic and anionic dyes) and fouling resistance (FRR is more than 90%). Moreover, this membrane performed excellent antibacterial activity (near about 3 log reduction) and chlorine tolerance. Thus the membrane can be a potential candidate for domestic as well as industrial application.

Supplementary Information

The online version contains supplementary material available at https://doi.org/10.1186/s42252-022-00032-w.

Additional file 1: Figure S1. FTIR Spectrum of dopamine and polydopamine. **Figure S2.** FTIR Spectrum of polystyrene (PS) and polystyrene sulfonate (PSS). Spectrum was taken over the range of 4000 to 400 cm^{-1} but for the analysis of sulfonic groups, Spectra are shown over the range from 1400 to 800 cm^{-1} (as in reference)[1]. **Figure S3.** FTIR Spectrum of PVDF membrane and NaOH treated PVDF membrane. **Figure S4.** Digital image of CFU of E. coli and S. aureus incubated on the control (a, c) and PSS-PDA-crosslinked GO membrane's surface (c, d).

Authors' contributions

SM has carried out the whole experiment and characterization, analyzed the data and drafted the manuscript. SB has edited the manuscript and provided intellectual inputs. The authors read and approved the final manuscript.

Availability of data and materials

All the data generated or analyzed during this study are included either in the main manuscript or in supporting information.

Declarations

Ethics approval and consent to participate

Not applicable.

References

1. Q. Bi, Q. Li, Y. Tian, Y. Lin, X. Wang, Hydrophilic modification of poly (vinylidene fluoride) membrane with poly (vinyl pyrrolidone) via a cross-linking reaction. J. Appl. Polym. Sci. **127**(1), 394–401 (2013)
2. D. Griggs, M. Stafford-Smith, O. Gaffney, J. Rockström, M.C. Öhman, P. Shyamsundar, W. Steffen, G. Glaser, N. Kanie, I. Noble, Sustainable development goals for people and planet. Nature **495**(7441), 305–307 (2013)
3. P.K. Samantaray, S. Baloda, G. Madras, S. Bose, A designer membrane tool-box with a mixed metal organic framework and RAFT-synthesized antibacterial polymer perform in tandem towards desalination, antifouling and heavy metal exclusion. J. Mater. Chem. A **6**(34), 16664–16679 (2018)
4. N. Scharnagl, H. Buschatz, Polyacrylonitrile (PAN) membranes for ultra- and microfiltration. Desalination **139**(1–3), 191–198 (2001)
5. C. De Fraiture, D. Molden, D. Wichelns, Investing in water for food, ecosystems, and livelihoods: An overview of the comprehensive assessment of water management in agriculture. Agric. Water Manag. **97**(4), 495–501 (2010)
6. Q. Long, J. Huang, S. Xiong, L. Shen, Y. Wang, Exploration of oligomeric sodium carboxylates as novel draw solutes for forward osmosis. Chem. Eng. Res. Des. **138**, 77–86 (2018)
7. Q. Long, Y. Jia, J. Li, J. Yang, F. Liu, J. Zheng, B. Yu, Recent advance on draw solutes development in forward osmosis. Processes **6**(9), 165 (2018)
8. Q. Long, G. Qi, Y. Wang, Evaluation of renewable gluconate salts as draw solutes in forward osmosis process. ACS Sustainable Chem. Eng. **4**(1), 85–93 (2016)
9. Q. Long, L. Shen, R. Chen, J. Huang, S. Xiong, Y. Wang, Synthesis and application of organic phosphonate salts as draw solutes in forward osmosis for oil–water separation. Environ. Sci. Technol. **50**(21), 12022–12029 (2016)
10. Q. Long, Y. Wang, Novel carboxyethyl amine sodium salts as draw solutes with superior forward osmosis performance. AIChE J. **62**(4), 1226–1235 (2016)
11. L. A. Hoover, W. A. Phillip, A. Tiraferri, N. Y. Yip, M. Elimelech, *Forward with osmosis: emerging applications for greater sustainability*. Environ. Sci. Technol. **45**(23), 9824-9830 (2011)
12. D.L. Shaffer, J.R. Werber, H. Jaramillo, S. Lin, M. Elimelech, Forward osmosis: where are we now? Desalination **356**, 271–284 (2015)
13. T.-S. Chung, S. Zhang, K.Y. Wang, J. Su, M.M. Ling, Forward osmosis processes: yesterday, today and tomorrow. Desalination **287**, 78–81 (2012)
14. S. Zhao, L. Zou, C.Y. Tang, D. Mulcahy, Recent developments in forward osmosis: opportunities and challenges. J. Membr. Sci. **396**, 1–21 (2012)
15. M. Stolov, V. Freger, Degradation of polyamide membranes exposed to chlorine: an impedance spectroscopy study. Environ. Sci. Technol. **53**(5), 2618–2625 (2019)
16. Q. Long, S. Zhao, J. Chen, Z. Zhang, G. Qi, Z.-Q. Liu, Self-assembly enabled nano-intercalation for stable high-performance MXene membranes. J. Membr. Sci. **635**, 119464 (2021)
17. G. Liu, J. Shen, Y. Ji, Q. Liu, G. Liu, J. Yang, W. Jin, Two-dimensional Ti 2 CT x MXene membranes with integrated and ordered nanochannels for efficient solvent dehydration. J. Mater. Chem. A **7**(19), 12095–12104 (2019)
18. A. Anand, B. Unnikrishnan, J.-Y. Mao, H.-J. Lin, C.-C. Huang, Graphene-based nanofiltration membranes for improving salt rejection, water flux and antifouling–A review. Desalination **429**, 119–133 (2018)
19. Y. Li, S. Li, K. Zhang, Influence of hydrophilic carbon dots on polyamide thin film nanocomposite reverse osmosis membranes. J. Membr. Sci. **537**, 42–53 (2017)
20. L. Shen, S. Xiong, Y. Wang, Graphene oxide incorporated thin-film composite membranes for forward osmosis applications. Chem. Eng. Sci. **143**, 194–205 (2016)
21. C. Zhang, K. Wei, W. Zhang, Y. Bai, Y. Sun, J. Gu, Graphene oxide quantum dots incorporated into a thin film nanocomposite membrane with high flux and antifouling properties for low-pressure nanofiltration. ACS Appl. Mater. Interfaces. **9**(12), 11082–11094 (2017)
22. X. Song, L. Wang, C.Y. Tang, Z. Wang, C. Gao, Fabrication of carbon nanotubes incorporated double-skinned thin film nanocomposite membranes for enhanced separation performance and antifouling capability in forward osmosis process. Desalination **369**, 1–9 (2015)
23. F. Shao, L. Dong, H. Dong, Q. Zhang, M. Zhao, L. Yu, B. Pang, Y. Chen, Graphene oxide modified polyamide reverse osmosis membranes with enhanced chlorine resistance. J. Membr. Sci. **525**, 9–17 (2017)
24. S. Zheng, Q. Tu, JJ. Urban, S. Li, B. Mi, Swelling of graphene oxide membranes in aqueous solution: characterization of interlayer spacing and insight into water transport mechanisms. ACS Nano. **11**(6), 6440–6450 (2017)
25. M. Zhang, Y. Mao, G. Liu, G. Liu, Y. Fan, W. Jin, Molecular bridges stabilize graphene oxide membranes in water. Angew. Chem. **132**(4), 1706–1712 (2020)
26. M. Zhang, K. Guan, Y. Ji, G. Liu, W. Jin, N. Xu, Controllable ion transport by surface-charged graphene oxide membrane. Nat. Commun. **10**(1), 1–8 (2019)
27. S. Liu, G. Zhou, K. Guan, X. Chen, Z. Chu, G. Liu, W. Jin, Dehydration of C2–C4 alcohol/water mixtures via electrostatically enhanced graphene oxide laminar membranes. AIChE J. **67**(6), aic17170 (2021)
28. G. Liu, W. Jin, N. Xu, Two-dimensional-material membranes: a new family of high-performance separation membranes. Angew. Chem. Int. Ed. **55**(43), 13384–13397 (2016)
29. F. Meng, F. Song, Y. Yao, G. Liu, S. Zhao, Ultrastable nanofiltration membranes engineered by polydopamine-assisted polyelectrolyte layer-by-layer assembly for water reclamation. ACS Sustainable Chem. Eng. **8**(29), 10928–10938 (2020)
30. K.L. Cho, A.J. Hill, F. Caruso, S.E. Kentish, Chlorine resistant glutaraldehyde crosslinked polyelectrolyte multilayer membranes for desalination. Adv. Mater. **27**(17), 2791–2796 (2015)
31. S. Maiti, P.K. Samantaray, S. Bose, In situ assembly of a graphene oxide quantum dot-based thin-film nanocomposite supported on de-mixed blends for desalination through forward osmosis. Nanoscale Adv. **2**(5), 1993–2003 (2020)
32. H. Saito, Y. Fujita, T. Inoue, Upper critical solution temperature behavior in poly (vinylidene fluoride)/poly (methyl methacrylate) blends. Polym. J. **19**(4), 405–412 (1987)
33. M. Sharma, G. Madras, S. Bose, Unique nanoporous antibacterial membranes derived through crystallization induced phase separation in PVDF/PMMA blends. J. Mater. Chem. A **3**(11), 5991–6003 (2015)
34. J.-H. Jiang, L.-P. Zhu, H.-T. Zhang, B.-K. Zhu, Y.-Y. Xu, Improved hydrodynamic permeability and antifouling properties of poly (vinylidene fluoride) membranes using polydopamine nanoparticles as additives. J. Membr. Sci. **457**, 73–81 (2014)
35. Y. Tran, P. Auroy, Synthesis of poly (styrene sulfonate) brushes. J. Am. Chem. Soc. **123**(16), 3644–3654 (2001)
36. P.K. Samantaray, G. Madras, S. Bose, Antibacterial and antibiofouling polymeric membranes through immobilization of pyridine derivative leading to ROS generation and loss in bacterial membrane integrity. ChemistrySelect **2**(26), 7965–7974 (2017)
37. S. Maiti, S. Bose, Free-standing graphene oxide membrane works in tandem with confined interfacial polymerization of polyamides towards excellent desalination and chlorine tolerance performance. Nanoscale Adv. **4**(2), 467–478 (2022)
38. M. Elimelech, W.H. Chen, J.J. Waypa, Measuring the zeta (electrokinetic) potential of reverse osmosis membranes by a streaming potential analyzer. Desalination **95**(3), 269–286 (1994)
39. N. Padmavathy, S.S. Behera, S. Pathan, L. Das Ghosh, S. Bose, Interlocked graphene oxide provides narrow channels for effective water desalination through forward osmosis. ACS Appl. Mater. Interfaces. **11**(7), 7566–7575 (2019)
40. E. Yang, C.-M. Kim, J.-H. Song, H. Ki, M.-H. Ham, I.S. Kim, Enhanced desalination performance of forward osmosis membranes based on reduced

graphene oxide laminates coated with hydrophilic polydopamine.
Carbon **117**, 293–300 (2017)

41. S. Kim, X. Lin, R. Ou, H. Liu, X. Zhang, G.P. Simon, C.D. Easton, H. Wang,
     Highly crosslinked, chlorine tolerant polymer network entwined gra-
     phene oxide membrane for water desalination. J. Mater. Chem. A **5**(4),
     1533–1540 (2017)
42. Q. Jia, Y. Li, Y. Liu, D. Duan, Layer-controlled synthesis of a silanol-graphene
     oxide nanosheet composite forward osmosis membrane by surface self-
     assembly. Langmuir **37**(27), 8095–8106 (2021)
43. D.M. Reurink, W.M. De Vos, H.D. Roesink, J. De Grooth, Polyelectrolyte
     multilayers for forward osmosis, combining the right multilayer and draw
     solution. Ind. Eng. Chem. Res. **60**(19), 7331–7341 (2021)

Publisher's Note

Springer Nature remains neutral with regard to jurisdictional claims in pub-
lished maps and institutional affiliations.